Parallel Transmission LiFi

Xiping Wu, *Member, IEEE*, and Dominic C. O'Brien, *Member, IEEE*

***Abstract*— Light fidelity (LiFi) is a relatively new wireless communication technology that exploits the optical spectrum. Compared to wireless fidelity (WiFi), LiFi is densely deployed with each access point (AP) covering an area only a few meters in diameter. Also, LiFi users are susceptible to intermittent light-path blockages. Meanwhile, the user is served by a single AP in conventional LiFi systems. This would cause frequent handovers for LiFi users, resulting in a degradation in quality of service. In this paper, parallel transmission is investigated for LiFi, which is named PT-LiFi. With a delicate design of the transmitter and the receiver, PT-LiFi enables multiple LiFi APs to serve the user simultaneously. Particularly, data transmission continues without interruption when the user is losing connectivity to some of the connected APs. Resource allocation is studied for the PT-LiFi system, and a novel load balancing method is proposed to jointly allocate resource across the APs. Results show PT-LiFi can make efficient use of the densely deployed LiFi APs and provide a flexible way of load balancing. Compared with a conventional LiFi system, the proposed method can increase user throughput by up to 150% and improve user fairness by up to 15%.**

***Index Terms*— Light fidelity (LiFi), parallel transmission, resource allocation, load balancing, user mobility, light-path blockage, handover.**

I. Introduction

LIGHT fidelity (LiFi) is a short-range wireless communication technology that uses light wave as signal bearers [1]. In contrast to the scarce and regulated radio frequency (RF) spectrum, the visible light spectrum is huge (about 300 THz) and unregulated. Other advantages that LiFi offers over wireless fidelity (WiFi) include: i) provision of illumination, ii) availability in RF-restricted areas, and iii) secure communication since light does not penetrate opaque structures [2]. More importantly, LiFi can provide high-speed data transmission to help fulfil the rapidly increasing demand for wireless communications. Recent research shows that with a single light-emitting diode (LED), LiFi is able to achieve peak data rates above 10 Gbps [3].

Compared to WiFi, LiFi supports a relatively small coverage area from a single access point (AP), typically an area 2-3 m in diameter [4]. This enables LiFi APs to be densely deployed. As a result, LiFi can offer very high area spectral efficiency, up to 1000 times as much as an RF femtocell [5]. However, frequent handovers may occur since users can quickly traverse the coverage area of a LiFi AP, even with a moderate speed. As frequent handovers would compromise user throughput, user mobility is non-negligible in access point selection (APS) and resource allocation (RA). Relevant research has been studied for LiFi and for hybrid LiFi and RF networks. In [6], a handover skipping scheme is reported, which enables the user to be transferred between two non-adjacent APs. Using the college admission model, a mobility-aware load balancing approach is developed for hybrid LiFi and long term evolution (LTE) networks in [7]. Another load balancing method based on fuzzy logic is proposed for hybrid LiFi and WiFi networks in [8]. In essence, these methods compromise the instantaneous data rate for a reduced handover rate.

Apart from user mobility, two other factors also influence the APS and RA process in LiFi. One factor is the receiver orientation. Due to a restricted field of view, the tilt of LiFi receivers would affect received signal strength (RSS). The closest AP might no longer provide the highest RSS. The randomness of LiFi receiver orientation is modelled in [9], and the corresponding impact on the handover rate is analysed in [10]. The other factor is the light-path blockage, which would result in a complete loss of connectivity [11]. In this case, the user needs to be transferred to another available AP until the light-path blockage ends. In [12], the APS issue in a hybrid LiFi and WiFi network is handled by measuring the handover cost caused by both user mobility and light-path blockages. Similar to [6]–[8], [12] also provides a trade-off between the instantaneous date rate and the handover rate.

However, the present APS and RA schemes for LiFi mostly consider that the user connects a single AP. This is restricted by the conventional transmission control protocol (TCP). Though these methods can improve the network performance of LiFi to some extent, they have two major limitations: i) a complete loss of throughput during handovers; and ii) a limited ability to balance traffic loads because each user can only acquire a portion of the resource of one AP. In contrast, multipath TCP (MPTCP) [14] enables the user to be served by multiple APs at the same time. This transmission mode is referred to as parallel transmission, with which data transmission can continue without interruption when the user is transferred between two APs. Studies have been carried out to investigate WiFi in an MPTCP context [15], [16]. In [15], an approach was proposed to cope with the issue that achievable throughput might reduce due to excessive connections over APs. This approach allows the user to freely use resources on its best WiFi path, while suppressing the use of other paths when congestion occurs. In [16], the impact

Manuscript received September 12, 2019; revised February 20, 2020 and May 30, 2020; accepted June 8, 2020. Date of publication June 19, 2020; date of current version October 9, 2020. This work was supported by the European Union's Horizon 2020 Research and Innovation Programme under Grant 825651 (ELIoT). The associate editor coordinating the review of this article and approving it for publication was G. Fodor. *(Corresponding author: Xiping Wu.)*

The authors are with the Department of Engineering Science, University of Oxford, Oxford OX1 3PJ, U.K. (e-mail: xiping.wu@eng.ox.ac.uk; dominic.obrien@eng.ox.ac.uk).

Color versions of one or more of the figures in this article are available online at http://ieeexplore.ieee.org.

Digital Object Identifier 10.1109/TWC.2020.3001983

TABLE I
DISTINCT POINTS

CoMP-based LiFi [13]	• LED panels reuse the same wavelengths of light • CoMP is used to mitigate interference at cell borders • LED panels jointly serve one user at a time • LED panels transmit the same information to one user
Parallel Transmission LiFi	• Neighbouring LED panels use different wavelengths of light • Frequency reuse is used to mitigate interference at cell borders • LED panels serve their users individually • LED panels transmit different information to one user

of controllable network parameters, e.g. the retransmission limit and buffer size, on the performance of MPTCP was analysed for joint WiFi and cellular network access. However, to the best knowledge of the authors, no research has so far been conducted to study parallel transmission for LiFi. When applying parallel transmission, LiFi differs from WiFi in two main points: i) due to the dense deployment, LiFi can provide more simultaneous connections than WiFi; and ii) LiFi is more susceptible to frequent handovers than WiFi. These points impose a two-sided impact on implementing parallel transmission for LiFi. On the one hand, LiFi could benefit from parallel transmission to a greater extent than WiFi. On the other hand, resource allocation becomes more challenging. Though load balancing in MPTCP has been widely discussed for wired networks [17], few studies have been done for wireless networks, of which the channel quality is varying. The work aforementioned in [15] addresses this issue for WiFi, but the method would fail in LiFi as its best path is not always available.

The main contribution of this paper is two-fold: i) a framework of parallel transmission is conceived for LiFi, including a delicate design of the transmitter and the receiver; and ii) a novel RA method is proposed to allocate the resource of LiFi APs in the parallel transmission system. Compared to the studies on applying coordinated multi-point (CoMP) transmission for LiFi, such as [13], the distinct points of our work are summarised in Table I. Performance simulations have been conducted for the proposed system with different numbers of connected APs. Results show that even with only two connected APs, parallel transmission can greatly improve the achievable throughput of LiFi over a single connected AP. It is also found that the proposed RA approach can significantly outperform the conventional method, especially when the user is served by more APs. The remainder of this paper is organised as follows. A framework of parallel transmission LiFi is demonstrated in Section II, including the transmitter, the receiver and the system model used for the investigation. The conventional RA method is introduced in Section III, while the novel RA method is proposed in Section IV. Simulation results are given in Section V. Finally, conclusions are drawn in Section VI.

II. FRAMEWORK OF PARALLEL TRANSMISSION LIFI

The parallel transmission LiFi (PT-LiFi) system considers an indoor wireless network that contains a number of LiFi APs. These APs are integrated into LED ceiling lamps facing downwards perpendicularly. They are arranged in a square lattice topology to model a regular lighting placement in an indoor scenario, e.g. an office. The APs reuse optical frequency bands and interfering signals are treated as noise. To fit for illumination purpose, each AP is composed of multiple LEDs with different wavelengths. The transmitter structure is provided in Section II-A. The receiver structure, which needs to separately receive data from different wavelengths, is introduced in Section II-B. The LiFi channel model is given in II-C, whereas the models of user mobility and light-path blockage are introduced in Section II-D and II-E. In PT-LiFi, the user is simultaneously served by multiple APs, and each pair of user and AP is called a subflow. The choice of subflows is discussed in Section II-F.

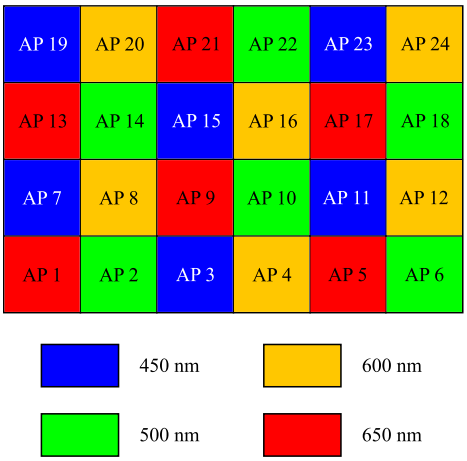

Fig. 1. The frequency reuse pattern used for the PT-LiFi system.

A. Transmitter Structure

Due to the nature of the square lattice deployment, the user is surrounded by four first-tier APs. Further APs are unlikely to provide a usable channel. Therefore, a frequency reuse (FR) factor of 4 is chosen, as shown in Fig. 1. Each AP is comprised by four colour LEDs RGBY (red, green, blue and yellow) [18] to meet the illumination requirement but uses only one of them for data transmission. Time-division multiple access (TDMA) is used for one AP to serve multiple users. Each user can be connected to a number of APs, between 1 and 4. The users of the room will see white light from each AP, and the illuminance will be set by the DC current fed to each LED. The communications will be achieved by modulating either R, G, B, Y at a level such that the average is correct so the overall illumination from the LED light is white. According to

TABLE II
PARAMETERS OF DIFFERENT WAVELENGTHS

Wavelength (nm)	**450**	**500**	**600**	**650**
Luminous efficacy L_{eff} (lm/W)	27	205	340	68
PD responsivity R_{pd} (A/W)	0.15	0.23	0.37	0.44
Intensity percentage ξ	10%	55%	20%	15%
Optical output power P_{out} (W)	9.3	6.7	1.5	5.5
Modulated optical power P_{mod} (W)	3.6	2.3	1.5	1.2

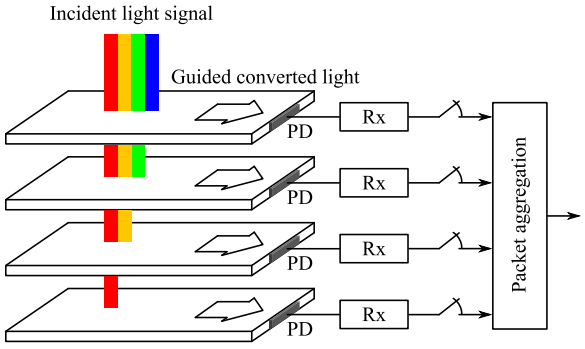

Fig. 2. The receiver structure with multilayer fluorescent concentrators.

the sRGB colour space,[1] 3:6:1 RGB and 4:5:1 YGB are adopted. The resulting intensity percentage of each modulated wavelength (which is denoted by ξ) is given in Table II. The luminous efficacy[2] (i.e. the ratio of luminous intensity to emitted optical power) and the photodiode (PD) responsivity are related to wavelength. These parameters are also listed in Table II.

Now we calculate the optical output power of each wavelength to meet illumination requirements. Let I_{lamp} and L_{eff} denote the lamp's illumination intensity and luminous efficacy, respectively. Assuming a 2.5 m separation between the two nearest APs, each AP covers an area of 6.25 m^2. To guarantee an illumination intensity of 400 lux, each lamp needs to provide $I_{\text{lamp}} = 400$ lux $\times$ 6.25 m^2 $= 2500$ lm. The optical output power of each modulated wavelength can be computed by $P_{\text{out}} = \frac{\xi I_{\text{lamp}}}{L_{\text{eff}}}$. To guarantee a non-negative optical signal, we have $P_{\text{mod}} \leq P_{\text{out}}$ for each wavelength. Yellow LEDs have the smallest $R_{\text{pd}}P_{\text{out}} = 0.54$ A. This value is chosen for all wavelengths to achieve the same signal-to-interference-plus-noise ratio (SINR) level for an equivalent RGBY channel. The modulated optical power can obtained by $P_{\text{mod}} = 0.54/R_{\text{pd}}$, which is shown in Table II.

B. Receiver Structure

At the receiver, signals carried by different wavelengths can be distinguished by placing optical filters in front of the PD. However, this approach requires a reception area proportional to the number of PDs. Alternatively, fluorescent concentrators [19] can be used, as shown in Fig. 2. Each concentrator converts the light of one wavelength to another and guides the converted light to a PD. By choice of concentrator material, it is possible to make the concentrator sensitive to a particular wavelength range. Since fluorescent concentrators are plain, they can be stacked to remain the same reception area. The concentrator gain g_c is formulated as [20, eq. (8)]:

$$g_c = \begin{cases} \dfrac{n^2}{\sin^2(\Psi_{\max})}, & 0 \leq \psi_{i,u} \leq \Psi_{\max} \\ 0, & \psi_{i,u} > \Psi_{\max} \end{cases}, \tag{1}$$

where n is the refractive index, $\Psi_{\max}$ is the semi-angle of the field of view (FoV) of the PD, and $\psi_{i,u}$ denotes the angle of incidence, which is the angle between the incident light and the receiver's orientation. This orientation can be determined by the azimuthal angle ω_u, which is uniformly distributed between 0 and 2π, and the polar angle θ_u, which follows a Laplace distribution with a mean of θ [9].

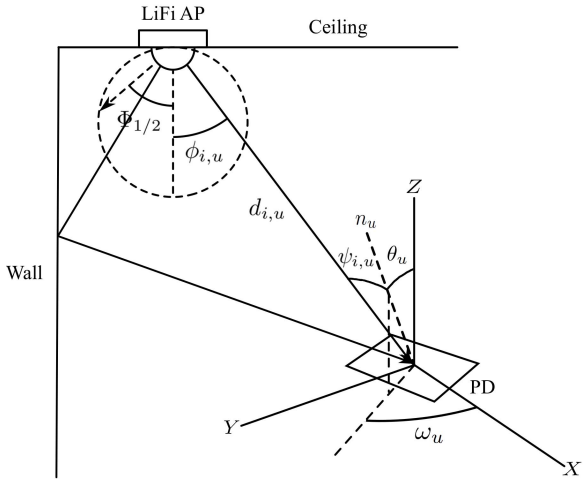

Fig. 3. The LoS and first-order NLoS paths of the LiFi channel.

C. Channel Model

A LiFi channel is comprised of two components: line-of-sight (LoS) and non line-of-sight (NLoS) paths, as shown in Fig. 3. The Euclidean distance of the LoS path between AP i and user u is denoted by $d_{i,u}$, with the same height assumed for all users. The LoS channel gain is denoted by $H_{i,u}^{\text{LoS}}$, which is given by [20, eq. (10)]:

$$H_{i,u}^{\text{LoS}} = \frac{(m+1)A_{\text{pd}}}{2\pi d_{i,u}^2} \cos^m(\phi_{i,u}) g_f g_c \cos(\psi_{i,u}), \tag{2}$$

where $m = -\ln 2/\ln(\cos\Phi_{1/2})$ represents the Lambertian emission order, and $\Phi_{1/2}$ is the angle of half intensity; A_{pd} is the physical area of the PD; $\phi_{i,u}$ denotes the angles of irradiance; and g_f is the optical filter gain.

Second-order reflections typically contribute little [20]. Thus, only first-order reflections are considered. A first-order reflection consists of two segments: a) from the AP to a small area w on the wall, and b) from w to the user. The Euclidean distances of these segments are denoted by $d_{i,w}$ and $d_{w,u}$. The angles of radiance and incidence with respect to the first

[1]The international commission on illumination (CIE) 1931 xy chromaticity diagram.

[2]From the response of a typical human eye to light that is standardised by the CIE in 1924.

segment are $\phi_{i,w}$ and $\vartheta_{i,w}$, and for the second segment they are $\vartheta_{w,u}$ and $\psi_{w,u}$. Let A_w denote the area of w. Let ρ_w denote the wall reflectivity. The channel gain of NLoS is denoted by $H_{i,u}^{\text{NLoS}}$, which is given by (3), shown at the bottom of this page, [6, eq. (3)].

The total gain of the LiFi channel is $H_{i,u} = H_{i,u}^{\text{LoS}} + H_{i,u}^{\text{NLoS}}$. The SINR of the link between AP i and user u can be expressed as follows:

$$\gamma_{i,u} = \frac{(R_{\text{pd}} H_{i,u} P_{\text{mod}})^2}{N_{\text{LiFi}} B_{\text{LiFi}} + \sum\limits_{j \in \mathcal{I}, j \neq i} (R_{\text{pd}} H_{j,u} P_{\text{mod}})^2}, \tag{4}$$

where N_{LiFi} denotes the power spectral density (PSD) of noise, which is assumed to be signal independent; B_{LiFi} is the bandwidth of the LiFi AP; $\mathcal{I}$ denotes the set of APs that use the same optical spectrum as AP i.

D. Mobility Model

There are a few studies investigating user mobility models for indoor scenarios, e.g. [21]. However, these studies are usually based on a specific floor plan that consists of compartments and corridors. In this paper, it is assumed that there are no compartments or corridors and users can move freely. To simulate the freely-moving users, the random waypoint (RWP) is adopted, which is a commonly used synthetic model for mobility [22]. Specifically, users move along a zigzag line from one waypoint to the next, with the waypoints being randomly distributed. With the original RWP model [23], the user moves around in a large outdoor area, e.g. a 1000 m by 1000 m region, and changes its speed when arriving at each waypoint. To suit an indoor scenario where the distance between two waypoints is relatively short, the user's speed is considered constant for a short period of time. The user's movement during such a period is called an excursion. When the current excursion finishes, the user chooses a new speed and continues moving. The user's speed is assumed to be uniformly distributed between 0 and $2v$, where v denotes the average speed.

E. Light-Path Blockage Model

There are two factors that affect the performance of a LiFi link when it is blocked: i) how often the blockage occurs; and ii) how long the blockage lasts. The first factor determines the handover rate caused by blockages, while the second influences the average user throughput. Accordingly, two parameters are used to characterise light-path blockages: the occurrence rate and occupation rate [12]. The occurrence rate, denoted by λ, is defined as the average number of blockages occurring in a time unit. This rate is assumed to follow the Poisson point process (PPP), which is usually used to model random events such as the arrival of packets at a switch [24]. The occupation rate, denoted by η, is defined as the proportion of time during which the user experiences blockages. We assume independent blockages among different APs. In practice, signals from different APs might be blocked due to a common obstacle. This can be reflected in the situation of a high occupation rate, where signals from multiple APs are likely to be blocked at the same time.

F. Choice of Subflows

A fixed number of subflows are considered, which are selected by following the rule of signal strength strategy (SSS), i.e. each user chooses a number of APs that provide the highest levels of SINR. A subflow could fail due to two situations: i) loss of connectivity and ii) traffic congestion. In the first situation, a handover can be implemented to let a new subflow join the current connection to ensure connectivity. In the second situation, two options are available. One option is replacing the congested subflow with another one. However, this might affect the APS results of other users and cause a chain reaction [25]. The other option is not to use the congested subflow and shift the traffic load to other subflows. This option is adopted in this work, since the congestion situations are comparable among APs under the assumption of uniformly distributed users.

III. Conventional Resource Allocation

The conventional RA method for LiFi copes with a single connected AP [26]. Applying this method to PT-LiFi is in fact to implement RA separately across APs. This method is hence referred to as autonomous resource allocation (ARA). A proportional fairness scheduler is considered, which is given by [27, eq. (9)]:

$$\max \sum_{u \in \mathbf{U}_i} \log(R_{i,u}), \tag{5}$$

where $R_{i,u}$ is the data rate that user u achieves from AP i (i and u denote the index of APs and the index of users throughput the paper), and $\mathbf{U}_i$ denotes the set of users served by AP i. The purpose of $\log(R_{i,u})$ is to reduce rewards for high data rates, while increasing penalties for low data rates. When $R_{i,u} = 0$, $\log(R_{i,u})$ would be negative infinity, invalidating the scheduler. Also, $R_{i,u} = 0$ would void the corresponding link between AP i and user u. Therefore, $R_{i,u} = 0$ is excluded from the possible solutions. Unlike conventional load balancing methods such as [28], ARA does not need to select the APs. Therefore, $R_{i,u}$ can be expressed as:

$$R_{i,u} = \rho_{i,u} r_{i,u}, \tag{6}$$

where $\rho_{i,u} \in (0, 1]$ denotes the proportion of time resource; and $r_{i,u}$ is the capacity of a LiFi link. The parameter $\gamma_{i,u}$ is an electrical SINR for non-negative signals, for which a tighter capacity bound can be found [29, eq. (37)]:

$$r_{i,u} = \frac{B_{\text{LiFi}}}{2} \log_2 \left(1 + \frac{e}{2\pi} \gamma_{i,u}\right). \tag{7}$$

$$H_{i,u}^{\text{NLoS}} = \int_{A_w} \frac{(m+1) A_{\text{pd}}}{2(\pi d_{i,w} d_{w,u})^2} \rho_w \cos^m(\phi_{i,w}) g_f g_c \cos(\psi_{w,u}) \cos(\vartheta_{i,w}) \cos(\vartheta_{w,u}) dA_w. \tag{3}$$

The sum of $\rho_{i,u}$ must not exceed 1. Thus, the ARA problem can be formulated as follows:

$$\begin{aligned} \max_{\rho_{i,u}} \quad & \sum_{u\in\mathbf{U}_i} \log(\rho_{i,u} r_{i,u}) \\ \text{s.t.} \quad & 0 < \rho_{i,u} \leq 1 \qquad \forall u \in \mathbf{U}_i; \\ & \sum_{u\in\mathbf{U}_i} \rho_{i,u} \leq 1. \end{aligned} \tag{8}$$

The problem in (8) can be readily solved by the Lagrangian multiplier method. Denoting the Lagrange multiplier by $\tilde{\lambda}$, the Lagrange function is written as:

$$\mathcal{L} = \sum_{u\in\mathbf{U}_i} \log\left(\rho_{i,u} r_{i,u}\right) - \tilde{\lambda}\left(\sum_{u\in\mathbf{U}_i} \rho_{i,u} - 1\right). \tag{9}$$

The solution of ARA is obtained by:

$$\rho_{i,u} = \frac{1}{N_{\mathbf{U}_i}}, \tag{10}$$

where $N_{\mathbf{U}_i}$ is the number of users that are served by AP i.

In addition to time resource, power can also be dynamically allocated among different users, with the average power being maintained to accommodate the illumination constraint. Relevant research has been studied in the current literature, e.g. [30] for VLC and [31] for a hybrid VLC and RF network. However, both studies consider a single VLC AP, without addressing co-channel interference (CCI). In this paper, multiple APs and the resulting CCI are taken into account, leading to enormous difficulties in optimising a joint time and power allocation. Moreover, this work is focused on investigating the benefits of parallel transmission to a LiFi system, against serial transmission. For these reasons, power allocation is not considered in this paper, and how power allocation can benefit PT-LiFi requires further research.

IV. Proposed Resource Allocation

In this section, a novel RA method is proposed for PT-LiFi. First, allocating resource across APs is formulated as a joint optimisation problem, namely joint resource allocation (JRA). Second, an iterative algorithm is proposed to reduce the computational complexity required for solving JRA. Finally, the optimality of the proposed algorithm is evaluated.

A. Joint Resource Allocation

Despite having multiple subflows, a user might still encounter poor link performance when light-path blockages occur to some subflows, especially those used to offer high-quality channels. This type of user needs more resource from the remaining subflows. This is however not supported by the ARA method. In order to realise proportional fairness for the users' overall data rates, the resource of APs needs to be jointly managed. The overall data rate of user u is $\sum_{i\in\mathbf{I}_u} \rho_{i,u} r_{i,u}$, where $\mathbf{I}_u$ denotes the set of APs that serve the user. Let $\mathbf{U}$ denote the set of all users that are connected to the LiFi network. The JRA problem can then be formulated as:

$$\begin{aligned} \max_{\rho_{i,u}} \quad & \sum_{u\in\mathbf{U}} \log\left(\sum_{i\in\mathbf{I}_u} \rho_{i,u} r_{i,u}\right) \\ \text{s.t.} \quad & 0 < \rho_{i,u} \leq 1 \qquad \forall i, u; \\ & \sum_{u\in\mathbf{U}_i} \rho_{i,u} \leq 1 \qquad \forall i. \end{aligned} \tag{11}$$

This is a nonlinear programming problem which can be solved by the OPTI toolbox [32]. However, this solution requires excessive computational complexity. A piece-wise linear approximation of the logarithmic function can be used to reformulate the problem as a linear programming [33]. Based on this, the authors in [34] proposed an iterative algorithm to solve network routing. However, as stated in Section III, an optimal solution of $\rho_{i,u}$ can be readily obtained with a single AP. Upon this, we propose an iterative algorithm to reduce computational complexity, without requiring a linear approximation of the logarithmic function.

B. Proposed Iterative Algorithm

With knowledge of the users' data rates that are provided by other APs, each AP can carry out resource allocation subsequently. The corresponding optimisation problem is written as:

$$\begin{aligned} \max_{\rho_{i,u}} \quad & \sum_{u\in\mathbf{U}_i} \log\left(\rho_{i,u} r_{i,u} + \sum_{j\in\mathbf{I}_u, j\neq i} \rho_{j,u} r_{j,u}\right) \\ \text{s.t.} \quad & 0 < \rho_{i,u} \leq 1 \qquad \forall u \in \mathbf{U}_i; \\ & \sum_{u\in\mathbf{U}_i} \rho_{i,u} \leq 1. \end{aligned} \tag{12}$$

Let $R_{\bar{i},u}$ denote the user's data rate that is provided by all APs except AP i, i.e. $R_{\bar{i},u} = \sum_{j\in\mathbf{I}_u, j\neq i} \rho_{j,u} r_{j,u}$. The Lagrange function for solving the above problem is expressed as:

$$\mathcal{L} = \sum_{u\in\mathbf{U}_i} \log\left(\rho_{i,u} r_{i,u} + R_{\bar{i},u}\right) - \tilde{\lambda}\left(\sum_{u\in\mathbf{U}_i} \rho_{i,u} - 1\right). \tag{13}$$

The optimal solution is obtained by:

$$\rho_{i,u} = \frac{1}{N_{\mathbf{U}_i}}\left[1 - \sum_{u'\in\mathbf{U}_i, u'\neq u}\left(\frac{R_{\bar{i},u}}{r_{i,u}} - \frac{R_{\bar{i},u'}}{r_{i,u'}}\right)\right]. \tag{14}$$

A variable $\delta_{i,u}$ is introduced to indicate the gap between the new $\rho_{i,u}$ and its previous value $\rho'_{i,u}$, i.e. $\delta_{i,u} = |\rho_{i,u} - \rho'_{i,u}|$. The set of all $\delta_{i,u}$ is denoted by $\boldsymbol{\delta}$. The iterations will stop if all elements of $\boldsymbol{\delta}$ are smaller than a preset target δ_{target}, i.e. $\min(\boldsymbol{\delta}) < \delta_{\text{target}}$. The pseudocode of the iterative algorithm is given in Algorithm 1. As can be observed from (14), the JRA method adapts to the instantaneous channel state, which affects channel capacity and thus the resource allocation results.

C. Optimality and Complexity Analysis

Due to the nature of the iterative algorithm, it is difficult to theoretically analyse its optimality. Alternatively, we experimentally study the optimality of the iterative algorithm by comparing it with the solutions provided by the OPTI toolbox.

Algorithm 1 Proposed Iterative Algorithm for JRA

Input: $\mathbf{I}_u$, $\mathbf{U}_i$, $r_{i,u}$ $\forall i \in \mathbf{I}_u, u \in \mathbf{U}_i$, δ_{target};
Output: $\rho_{i,u}$;
Initialisation: $R_{\bar{i},u} \leftarrow 0$;
while $\max(\boldsymbol{\delta}) \geq \delta_{\text{target}}$ **do**
for each AP i **do**
for each user $u \in \mathbf{U}_i$ **do**

$$\rho'_{i,u} = \rho_{i,u};$$

$$\rho_{i,u} = \frac{1}{N_{\mathbf{U}_i}} \left[1 - \sum_{u' \in \mathbf{U}_i, u' \neq u} \left(\frac{R_{\bar{i},u}}{r_{i,u}} - \frac{R_{\bar{i},u'}}{r_{i,u'}} \right) \right];$$

$$\delta_{i,u} = |\rho_{i,u} - \rho'_{i,u}|;$$

end for
end for
end while
return $\rho_{i,u}$ $\forall i \in \mathbf{I}_u, u \in \mathbf{U}_i$

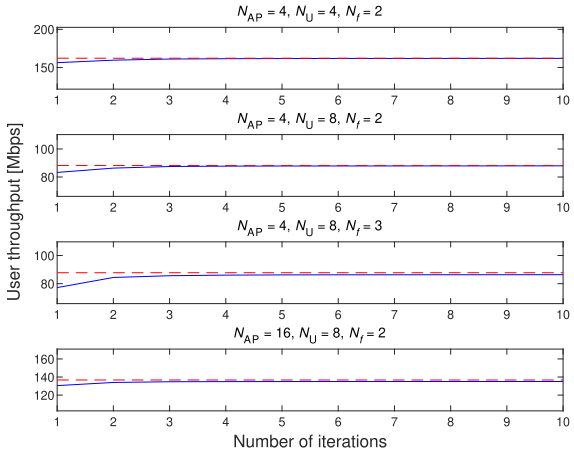

Fig. 4. User throughput versus the number of iterations (solid line: the proposed iterative algorithm; dashed line: the optimal solution provided by the OPTI toolbox).

Since JRA provides an RA solution for a given time instant, user mobility and light-path blockages are not considered here. See the detailed setup in Section V. Let N_{AP}, $N_{\mathbf{U}}$ and N_f denote the number of APs, the number of users and the number of subflows, respectively. For different N_{AP}, $N_{\mathbf{U}}$ and N_f, Fig. 4 shows the achieved throughput of the iterative algorithm as a function of the number of iterations in solid lines. The solutions provided by the OPTI toolbox are represented by dashed lines. As shown, the proposed algorithm reaches a steady state within 4 iterations and achieves a near-optimal throughput, within 2%.

For each iteration, the proposed algorithm calculates $\rho_{i,u}$ for each subflow. The order of complexity is the total number of subflows, which is $N_{\mathbf{U}}N_f$. Using 4 iterations, the proposed algorithm has an order of complexity of $4N_{\mathbf{U}}N_f$. As for the optimal solutions for JRA, the computational complexity can be estimated by discretizing the time resource of each AP into N_t portions. Each portion is allocated to one of the subflows associated to the AP. Since there are $N_{\mathbf{U}}N_f$ subflows in total, each AP has $\frac{N_{\mathbf{U}}N_f}{N_{\text{AP}}}$ in average. Thus, the optimal solution has an order of complexity of $(N_{\text{AP}}N_t)^{\frac{N_{\mathbf{U}}N_f}{N_{\text{AP}}}}$. Taking $N_{\text{AP}} = 8$, $N_{\mathbf{U}} = 8$, $N_f = 4$ and $N_t = 20$ for an example, the proposed algorithm can reduce computational complexity in an order of magnitude of 7 against the optimal solution.

TABLE III
SIMULATION PARAMETERS

Parameter	Value
Room size (length by width by height)	10 m × 10 m × 3 m
Physical area of the PD, A_{pd}	1 cm^2
Gain of the optical filter, g_f	1
Refractive index, n	1.5
Half-intensity radiation angle, $\Phi_{1/2}$	60°
FoV semi-angle of the receiver, $\Psi_{\max}$	90°
Modulated optical power, P_{opt}	See Table II
Detector responsivity, R_{pd}	See Table II
Bandwidth per LiFi AP, B_{LiFi}	20 MHz
PSD of noise in LiFi, N_{LiFi}	10^{-21} A^2/Hz [35]

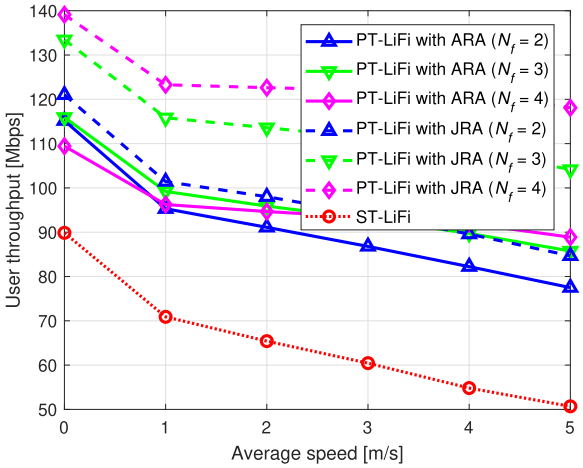

Fig. 5. User throughput versus the user's average speed ($\theta = 0°$, $\lambda = 0$ /min, and $N_{\mathbf{U}} = 10$).

V. SIMULATION RESULTS

In this section, results are reported from Monte Carlo simulations carried out to evaluate the performance of PT-LiFi. The JRA method is implemented through the iterative algorithm with 5 iterations. The baseline is a conventional LiFi system which uses a single connected AP. Such a system is referred to as ST-LiFi. We consider 16 APs, with a 2.5m separation between the two nearest APs. The handover overhead is set to be 200 ms [36], and no data transmission is available during the handover process. Other parameters are listed in Table III. The simulations measure the achievable data rate of the LiFi network through the capacity bound in (7). For each situation 1000 simulations are run, with each simulation lasting a period of 100s.

A. Effects of User Mobility

Fig. 5 shows user throughput as a function of the user's speed, with perpendicular receiver orientations and no light-path blockages. As shown, PT-LiFi with just 2 subflows can greatly outperform ST-LiFi. In the extreme case of stationary

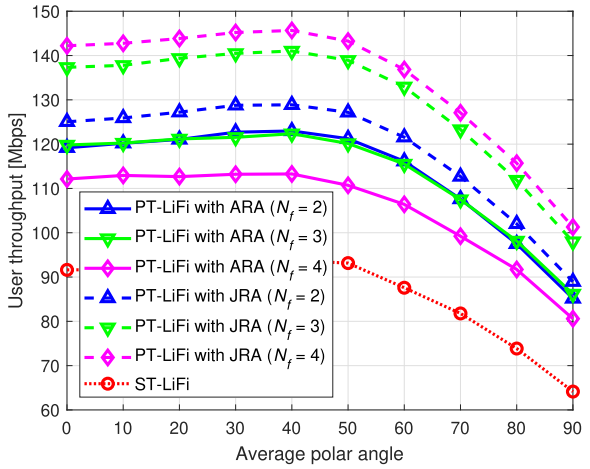

Fig. 6. User throughput versus the average polar angle ($v = 0$ m/s, $\lambda = 0$ /min, and $N_{\mathbf{U}} = 10$).

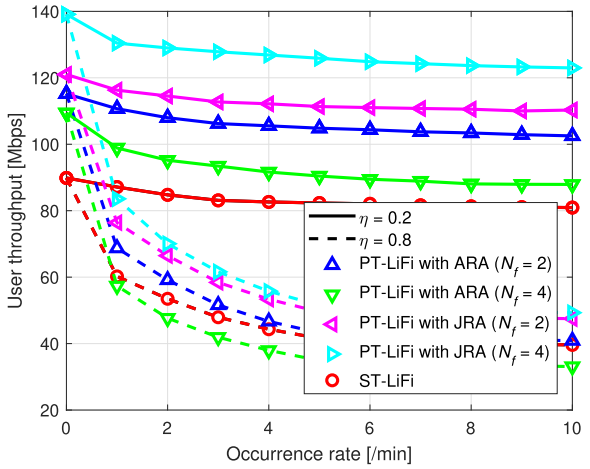

Fig. 7. User throughput versus the occurrence rate ($v = 0$ m/s, $\theta = 0°$, and $N_{\mathbf{U}} = 10$).

users, ARA and JRA with $N_f = 2$ obtain user throughputs of 115 Mbps and 121 Mbps, which are 28% and 34% higher than the 90 Mbps obtained by ST-LiFi. It is also found that the throughput of JRA monotonically increases with N_f, whereas the throughput of ARA does not. This is because JRA can balance traffic loads across subflows and more subflows provide a higher flexibility of load balancing. As for ARA, the reason for the trend is two-fold. On the one hand, adding a subflow of poor channel to one user would harm the interests of other users that are served by the same AP. On the other hand, more subflows can compensate the throughput loss due to frequent handovers caused by fast-moving users. Hence, for ARA, $N_f = 4$ performs worse than $N_f = 2$ when $v = 0$ m/s, but otherwise when $v = 5$ m/s. This makes JRA outperform ARA more significantly when N_f increases, by up to 33%. Furthermore, PT-LiFi surpasses ST-LiFi more greatly when the users move faster. Taking $N_f = 4$ as an example, the throughput gap between JRA and ST-LiFi is 49 Mbps for $v = 0$ m/s. This gap increases to 67 Mbps when $v = 5$ m/s, 133% higher than ST-LiFi. This is because when one subflow is being transferred between APs, PT-LiFi can use the remaining subflows for data transmission.

B. Effects of Receiver Orientation

Fig. 6 presents the impact of receiver orientation with different values of the average polar angle θ. The users are stationary with no light-path blockages. As θ increases, the user throughput increases slightly until $\theta = 40°$ and then decreases rapidly. The slight increase is because a moderate θ can mitigate interference to some extent, whereas the rapid decrease is due to the difficulty in receiving lights with a large θ. PT-LiFi noticeably outperforms ST-LiFi, with an almost stable gap between them for different θ. For instance, ARA with $N_f = 2$ achieves 30% more throughput than ST-LiFi when $\theta = 0°$, and 33% when $\theta = 90°$. As N_f increases, the user throughput of ARA decreases for the reasons explained above. In contrast, JRA provides a substantial benefit when N_f increases. When $\theta = 90°$, for example, JRA achieves 89 Mbps with $N_f = 2$ and 98 Mbps with $N_f = 3$, which are 39% and 53% more than ST-LiFi, respectively.

C. Effects of Light-Path Blockage

In Fig. 7, the user throughput is shown as a function of the occurrence rate of light-path blockages. Two occupation rates, 0.2 and 0.8, are demonstrated. The occurrence rate λ and the occupation rate η degrade throughput performance in separate ways. As shown, the user throughput decreases for all methods when λ increases, since frequent light-path blockages result in frequent handovers. Given a particular value of λ, the throughput performance deteriorates much more rapidly when $\eta = 0.8$ than $\eta = 0.2$. The reason lies in the worsened channel quality during light-path blockages. In an extreme case of $\eta = 1$, all approaches would deliver zero throughput. This also explains the phenomenon that PT-LiFi only provides a marginal gain over ST-LiFi when $\eta = 0.8$. At $\lambda = 10$ /min with $\eta = 0.2$, JRA (with $N_f = 4$) and ST-LiFi achieve 123 Mbps and 81 Mbps, respectively. When $\eta = 0.8$, these throughputs decrease to 50 Mbps and 40 Mbps, respectively.

D. Effects of the Number of Users

The effects of the number of users in a practical scenario are analysed. The average walking speed of people is 1.4 m/s, and the average polar angle while walking is about 30° [9]. Light-path blockages are assumed to occur once per minute, with an occupation rate of 0.1. The relation between user throughput and the number of users $N_{\mathbf{U}}$ is presented in Fig. 8. For all methods, the user throughput decreases as $N_{\mathbf{U}}$ increases, as expected from the limited system capacity. However, the throughput of PT-LiFi decreases more rapidly than that of ST-LiFi, leading to a smaller gain for a larger $N_{\mathbf{U}}$. For instance, ARA with $N_f = 4$ achieves a throughput about 153% more than ST-LiFi when $N_{\mathbf{U}} = 1$, while only 30% when $N_{\mathbf{U}} = 10$. This indicates that PT-LiFi can improve network performance more significantly when serving fewer users. It is also found that JRA acquires a larger gain over ARA as $N_{\mathbf{U}}$ increases. This is because when $N_{\mathbf{U}}$

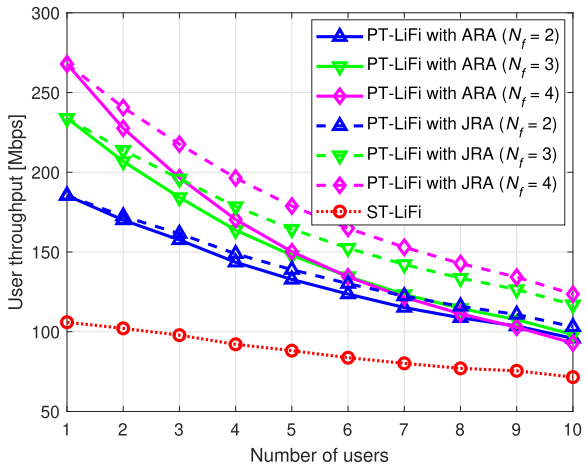

Fig. 8. User throughput versus the number of users ($v = 1.4$ m/s, $\theta = 30°$, $\lambda = 1$ /min, $\eta = 0.1$).

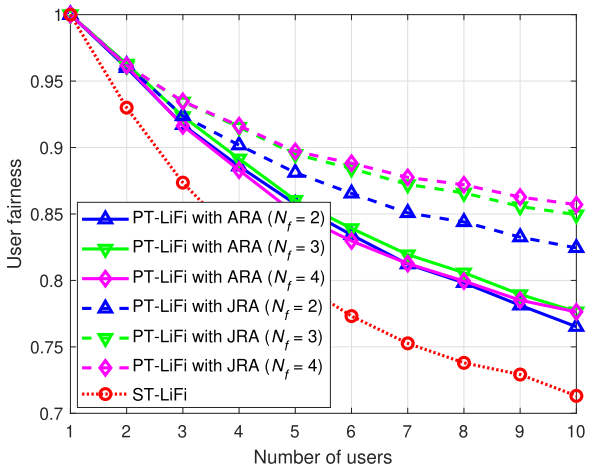

Fig. 9. User fairness versus the number of users ($v = 1.4$ m/s, $\theta = 30°$, $\lambda = 1$ /min, $\eta = 0.1$).

increases, JRA can implement load balancing more flexibly than ARA.

E. User Fairness

User fairness is measured in the same scenario as above. Jain's fairness index is adopted, which is given by [37, eq. (14)]:

$$\chi = \frac{\left(\sum_{u=1}^{N_{\mathbf{U}}} R_u\right)^2}{N_{\mathbf{U}} \sum_{u=1}^{N_{\mathbf{U}}} R_u^2}, \tag{15}$$

where R_u is the achieved throughput of user u.

As shown in Fig. 9, PT-LiFi achieves a much higher user fairness than ST-LiFi, especially for a large number of users. This is because PT-LiFi can flexibly allocate resource through multiple subflows. Taking $N_{\mathbf{U}} = 10$ as an example, ARA with $N_f = 4$ reaches a user fairness of 78%, whereas ST-LiFi only provides 71%. Meanwhile, JRA is able to elevate the user fairness to 86%, which is 15% higher than ST-LiFi.

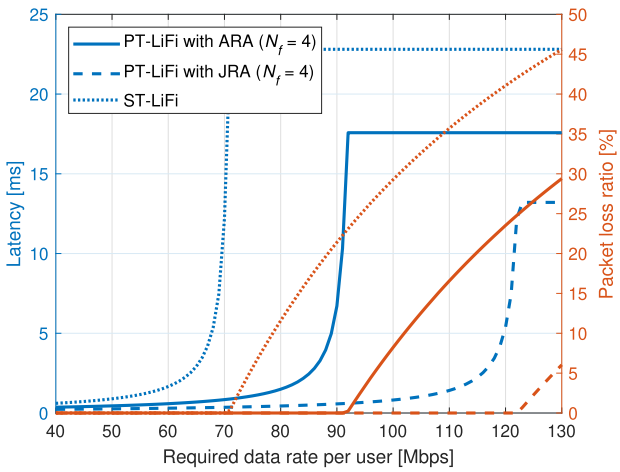

Fig. 10. Latency and packet loss ratio ($N_{\mathbf{U}} = 10$, $v = 1.4$ m/s, $\theta = 30°$, $\lambda = 1$ /min, $\eta = 0.1$).

F. Latency and Packet Loss Ratio

Finally, we study the network performance in terms of latency and packet loss ratio. The packet size is 1500 bytes, and the buffer size is set to be 128K bytes. The normalized buffer size is denoted by N_B, which equals the buffer size divided by the packet size. Based on the measured AP capacity, the average number of packets queueing in one AP can be estimated by Little's law: $N_W = \frac{\tilde{R}}{R - \tilde{R}}$, where R denotes the AP capacity and $\tilde{R}$ is the required data rate. Packet loss occurs when N_W exceeds N_B. The latency is obtained by $\frac{\min\{N_W, N_B\}}{\min\{R, \tilde{R}\}}$. As shown in Fig. 10, ST-LiFi can only support 52 Mbps per user when achieving a latency requirement below 1 ms. Meanwhile, PT-LiFi with JRA can provide 105 Mbps, which is twice as fast as ST-LiFi. In addition, ST-LiFi starts losing packets when the the required data rate reaches 73 Mpbs, while JRA remains a zero packet loss ratio until 122 Mpbs.

VI. Conclusion

In this paper, parallel transmission was investigated for LiFi and a novel RA method named JRA was proposed. Unlike ST-LiFi, PT-LiFi enables the user to be served by multiple APs simultaneously, making an efficient use of the densely-deployed LiFi APs. Compared with ST-LiFi, PT-LiFi can improve network performance in two aspects: i) providing a flexible way of load balancing; and ii) mitigating the throughput loss caused by handovers. The performance of the proposed system, in terms of user throughput and fairness, was comprehensively studied by considering user mobility, random receiver orientation and light-path blockages. Results show that even with just 2 subflows, PT-LiFi can greatly improve network performance against ST-LiFi. In addition, the proposed JRA achieves a higher throughput as well as user fairness than ARA, especially for a larger number of subflows. With 4 subflows, JRA can enable PT-LiFi to increase user throughput over ST-LiFi by up to about 150%, while improving user fairness by up to 15%.

REFERENCES

[1] H. Haas, L. Yin, Y. Wang, and C. Chen, "What is LiFi?" *J. Lightw. Technol.*, vol. 34, no. 6, pp. 1533–1544, Mar. 15, 2016.

[2] L. Hanzo, H. Haas, S. Imre, D. O'Brien, M. Rupp, and L. Gyongyosi, "Wireless myths, realities, and futures: From 3G/4G to optical and quantum wireless," *Proc. IEEE*, vol. 100, no. Special Centennial Issue, pp. 1853–1888, May 2012.

[3] M. S. Islim *et al.*, "Towards 10 Gb/s orthogonal frequency division multiplexing-based visible light communication using a GaN violet micro-LED," *Photon. Res.*, vol. 5, no. 2, p. A35, Apr. 2017.

[4] H. Haas, "Visible light communication," in *Proc. Opt. Fiber Commun. Conf. Exhib. (OFC)*, Los Angeles, CA, USA, 2015, pp. 1–72.

[5] I. Stefan, H. Burchardt, and H. Haas, "Area spectral efficiency performance comparison between VLC and RF femtocell networks," in *Proc. IEEE Int. Conf. Commun. (ICC)*, Budapest, Hungary, Jun. 2013, pp. 3825–3829.

[6] X. Wu and H. Haas, "Handover skipping for LiFi," *IEEE Access*, vol. 7, pp. 38369–38378, 2019.

[7] L. Li, Y. Zhang, B. Fan, and H. Tian, "Mobility-aware load balancing scheme in hybrid VLC-LTE networks," *IEEE Commun. Lett.*, vol. 20, no. 11, pp. 2276–2279, Nov. 2016.

[8] Y. Wang, X. Wu, and H. Haas, "Fuzzy logic based dynamic handover scheme for indoor Li-Fi and RF hybrid network," in *Proc. IEEE Int. Conf. Commun. (ICC)*, Kuala Lumpur, Malaysia, May 2016, pp. 1–6.

[9] M. D. Soltani, A. A. Purwita, Z. Zeng, H. Haas, and M. Safari, "Modeling the random orientation of mobile devices: Measurement, analysis and LiFi use case," *IEEE Trans. Commun.*, vol. 67, no. 3, pp. 2157–2172, Mar. 2019.

[10] M. D. Soltani, H. Kazemi, M. Safari, and H. Haas, "Handover modeling for indoor Li-Fi cellular networks: The effects of receiver mobility and rotation," in *Proc. IEEE Wireless Commun. Netw. Conf. (WCNC)*, San Francisco, CA, USA, Mar. 2017, pp. 1–6.

[11] S. Jivkova and M. Kavehrad, "Shadowing and blockage in indoor optical wireless communications," in *Proc. IEEE Global Telecommun. Conf. (GLOBECOM)*, San Francisco, CA, USA, vol. 6, Dec. 2003, pp. 3269–3273.

[12] X. Wu and H. Haas, "Access point assignment in hybrid LiFi and WiFi networks in consideration of LiFi channel blockage," in *Proc. IEEE 18th Int. Workshop Signal Process. Adv. Wireless Commun. (SPAWC)*, Sapporo, Japan, Jul. 2017, pp. 1–5.

[13] A. A. Dowhuszko and A. I. Perez-Neira, "Achievable data rate of coordinated multi-point transmission for visible light communications," in *Proc. IEEE 28th Annu. Int. Symp. Pers., Indoor, Mobile Radio Commun. (PIMRC)*, Montreal, QC, Canada, Oct. 2017, pp. 1–7.

[14] A. Ford, C. Raiciu, M. Handley, and O. Bonaventure, *TCP Extensions for Multipath Operation With Multiple Addresses*, document RFC 6824, Fremont, CA, USA, Jan. 2013.

[15] M. R. Palash and K. Chen, "MPWiFi: Synergizing MPTCP based simultaneous multipath access and WiFi network performance," *IEEE Trans. Mobile Comput.*, vol. 19, no. 1, pp. 142–158, Jan. 2020.

[16] S. R. Pokhrel and M. Mandjes, "Improving multipath TCP performance over WiFi and cellular networks: An analytical approach," *IEEE Trans. Mobile Comput.*, vol. 18, no. 11, pp. 2562–2576, Nov. 2019.

[17] A. Jerome, M. Yuksel, S. H. Ahmed, and M. Bassiouni, "SDN-based load balancing for multi-path TCP," in *Proc. IEEE INFOCOM-IEEE Conf. Comput. Commun. Workshops (INFOCOM WKSHPS)*, Honolulu, HI, USA, Apr. 2018, pp. 859–864.

[18] T. H. Loh *et al.*, "Link performance evaluation of 5G mm-wave and LiFi systems for the transmission of holographic 3D display data," in *Proc. 13th Eur. Conf. Antennas Propag. (EuCAP)*, Kraków, Poland, 2019, pp. 1–4.

[19] P. P. Manousiadis *et al.*, "Wide field-of-view fluorescent antenna for visible light communications beyond the étendue limit," *Optica*, vol. 3, no. 7, pp. 702–706, Sep. 2016.

[20] J. M. Kahn and J. R. Barry, "Wireless infrared communications," *Proc. IEEE*, vol. 85, no. 2, pp. 265–298, Feb. 1997.

[21] L. Subrt, P. Pechac, O. Hrstka, V. Micka, and J. Vokrinek, "Novel mobility model for indoor conference scenarios," in *Proc. 8th Eur. Conf. Antennas Propag. (EuCAP)*, The Hague, The Netherlands, Apr. 2014, pp. 2136–2137.

[22] D. Johnson and D. Maltz, "Dynamic source routing in ad hoc wireless networks," in *Mobile Computing*. Dordrecht, The Netherlands: Kluwer, 1996, pp. 153–181.

[23] W. Navidi and T. Camp, "Stationary distributions for the random waypoint mobility model," *IEEE Trans. Mobile Comput.*, vol. 3, no. 1, pp. 99–108, Jan. 2004.

[24] L. Kleinrock, *Queueing Systems: Theory*. West Sussex, U.K.: Wiley, 1976.

[25] Y. Wang, X. Wu, and H. Haas, "Load balancing game with shadowing effect for indoor hybrid LiFi/RF networks," *IEEE Trans. Wireless Commun.*, vol. 16, no. 4, pp. 2366–2378, Apr. 2017.

[26] D. Bykhovsky and S. Arnon, "Multiple access resource allocation in visible light communication systems," *J. Lightw. Technol.*, vol. 32, no. 8, pp. 1594–1600, Apr. 15, 2014.

[27] X. Wu, M. Safari, and H. Haas, "Joint optimisation of load balancing and handover for hybrid LiFi and WiFi networks," in *Proc. IEEE Wireless Commun. Netw. Conf. (WCNC)*, San Francisco, CA, USA, Mar. 2017, pp. 1–5.

[28] X. Li, R. Zhang, and L. Hanzo, "Cooperative load balancing in hybrid visible light communications and WiFi," *IEEE Trans. Commun.*, vol. 63, no. 4, pp. 1319–1329, Apr. 2015.

[29] J.-B. Wang, Q.-S. Hu, J. Wang, M. Chen, and J.-Y. Wang, "Tight bounds on channel capacity for dimmable visible light communications," *J. Lightw. Technol.*, vol. 31, no. 23, pp. 3771–3779, Dec. 1, 2013.

[30] A. M. Abdelhady, O. Amin, A. Chaaban, and M.-S. Alouini, "Downlink resource allocation for multichannel TDMA visible light communications," in *Proc. IEEE Global Conf. Signal Inf. Process. (GlobalSIP)*, Washington, DC, USA, Dec. 2016, pp. 1–5.

[31] V. K. Papanikolaou, P. D. Diamantoulakis, P. C. Sofotasios, S. Muhaidat, and G. K. Karagiannidis, "On optimal resource allocation for hybrid VLC/RF networks with common backhaul," *IEEE Trans. Cognit. Commun. Netw.*, vol. 6, no. 1, pp. 352–365, Mar. 2020.

[32] *OPTI Toolbox V2.28*. Accessed: Apr. 6, 2019. [Online]. Available: https://www.inverseproblem.co.nz/OPTI/

[33] B. Fortz and M. Thorup, "Internet traffic engineering by optimizing OSPF weights," in *Proc. Conf. Comput. Commun. 19th Annu. Joint Conf. IEEE Comput. Commun. Societies (IEEE INFOCOM)*, Tel Aviv-Yafo, Israel, vol. 2, 2000, pp. 519–528.

[34] E.-S.-M. El-Alfy, S. N. Mujahid, and S. Z. Selim, "A Pareto-based hybrid multiobjective evolutionary approach for constrained multipath traffic engineering optimization in MPLS/GMPLS networks," *J. Netw. Comput. Appl.*, vol. 36, no. 4, pp. 1196–1207, Jul. 2013.

[35] D. A. Basnayaka and H. Haas, "Hybrid RF and VLC systems: Improving user data rate performance of VLC systems," in *Proc. IEEE 81st Veh. Technol. Conf. (VTC Spring)*, Glasgow, Scotland, May 2015, pp. 1–5.

[36] J. Xiao and F. Liu, "A pre-scanning fast handoff scheme for VoIP in WLANs," *Int. J. Future Comput. Commun.*, vol. 8, no. 2, pp. 343–354, 2015.

[37] X. Wu, M. Safari, and H. Haas, "Access point selection for hybrid Li-Fi and Wi-Fi networks," *IEEE Trans. Commun.*, vol. 65, no. 12, pp. 5375–5385, Dec. 2017.

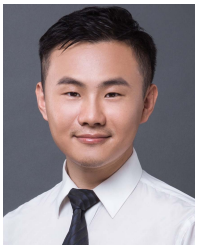

Xiping Wu (Member, IEEE) received the Ph.D. degree from The University of Edinburgh, U.K., in 2015. From 2011 to 2014, he was a Marie–Curie Early-Stage Researcher, funded by the European Union's Seventh Framework Program (FP7). From 2015 to 2018, he held a Post-Doctoral Fellowship with The University of Edinburgh, funded by the British Engineering and Physical Sciences Research Council (EPSRC). He is currently a Research Fellow with the University of Oxford. He has authored or coauthored over 40 journal articles and conference papers. His main research interests include optical wireless communications, hybrid OWC and RF networks, and the Internet of Things.

Dominic C. O'Brien (Member, IEEE) is a Professor of engineering science with the University of Oxford and leads the Optical Communications Group. He is also the Director of the U.K. Quantum Technology Hub in Quantum Computing and Simulation. He has a range of experience in optoelectronics research in industry (BT Labs) and academia, and has authored or coauthored approximately 200 publications in this area. His group has a wide range of experience in free-space optical communications and optical wireless communications, demonstrating integrated optical wireless transceivers, full room-scale systems at 300 Mbit/s, and integrated visible light communications systems.